

RESEARCH PAPER

## Solubility and Dissolution Properties of Generic Rifampicin Raw Materials

S. Q. Henwood, M. M. de Villiers,\* W. Liebenberg, and A. P. Lötter

Research Institute for Industrial Pharmacy, Potchefstroom University for Christian Higher Education, Potchefstroom, 2520, South Africa

### ABSTRACT

*Rifampicin shows polymorphism; therefore, it is necessary to select a suitable crystal form at an early stage of development to ensure optimum solubility and dissolution rates. This study was an investigation into the crystal properties of several rifampicin raw materials currently being used by manufacturers of generic rifampicin raw materials in South Africa. Powders were characterized by X-ray diffraction (XRD), infrared (IR) spectroscopy, and differential scanning calorimetry (DSC). The solubility in water and dissolution properties in water, buffer pH 7.4 and 0.1 M HCl, were also measured. The main difference between the powders was the amorphous content. XRD, IR, and DSC methods could detect the presence of amorphous rifampicin. In contrast to expectations, an increase in amorphous content significantly reduced the dissolution rate of the powders in water and buffer pH 7.4. This behavior was attributed to the electrostatic properties of the very fine particles in the amorphous powders. The results of this study showed that the physical properties of rifampicin raw materials varied not only among manufacturers, but also among batches from the same manufacturer.*

**Key Words:** Dissolution; Generic; Powders; Rifampicin; Solubility.

### INTRODUCTION

Rifampicin (BP), also called rifampin (USP), is a major drug of choice in the treatment of tuberculosis and leprosy. Bioinequivalency has been reported for mar-

keted products of rifampicin (1). Dissolution, and therefore bioavailability, depends on the crystal properties of a drug. Rifampicin shows polymorphism, which is believed to be due to the various possibilities for hydrogen bonding, conformational exchanges, and ionization

\* To whom correspondence should be addressed.

states, which allow different crystalline packing of the complex structure to occur (2). Therefore, it is necessary to select a suitable crystal form of rifampicin at an early stage of development to ensure optimum solubility and dissolution rates (3).

Solubility and dissolution also depend on the particle size of a drug. Jindal et al. studied the effect of particle size on the bioavailability and dissolution of rifampicin (4). They found that particle size had no significant effect on the absorption of this drug. However, when the drug is very fine (mean particle size  $\leq 10 \mu\text{m}$ ), the presence of electrostatic forces may result in lump formation and subsequent delayed dissolution and poor bioavailability.

This study was prompted by several failures in dissolution equivalency of rifampicin products manufactured in South Africa. On visual inspection of the raw material samples used to manufacture these products, it was evident that the powders had definite differences in their particle sizes and shapes. This led to an investigation into the crystal properties of several rifampicin raw materials available to manufacturers of generic products in South Africa.

## EXPERIMENTAL

### Materials

All solvents were analytical grade, and water appropriate for liquid chromatography was used. Rifampicin powders (Rifampin, USP), which are currently used to manufacture rifampicin-containing products, were obtained randomly from three suppliers: Marshing (Marshing and Company Africa [PTY] Limited, Johannesburg, South Africa), batch number (BN) 940538, 6995, and Rin 95/079; Themis (Themis Chemicals Limited, Bombay, India), BN RD 95195; and Yuhan (Yuhan Corporation, Seoul, Korea), BN 4060.

### Scanning Electron Microscopy

A scanning electron microscope (SEM; Philips XL 30, Eindhoven, Netherlands) was used to obtain photomicrographs of the different crystal forms. Samples were mounted on a metal stub with an adhesive and coated under vacuum with carbon (Emscope TB500 sputter-coater, Cambridge, England) before being coated with a thin gold-platinum film (Eiko Engineering Ion Coater IB-2, Tokyo, Japan).

### Infrared Analysis

Samples weighing approximately 2 mg were mixed with 200 mg spectral grade KBr (Merck, Germany) by

means of an agate mortar and pestle. Disks were pressed using a Beckman 00-25 press (Beckman, Fullerton, CA) at  $15 \times 10^5 \text{ kg/cm}^2$ . A Shimadzu FTIR-4200 spectrometer (Shimadzu, Kyoto, Japan) was used to obtain infrared (IR) spectra in the range  $4000\text{--}400 \text{ cm}^{-1}$ . IR spectra were also obtained using a diffuse reflectance attachment to the FTIR (Fourier transform infrared) spectrometer (DRFTIR).

### X-Ray Powder Diffractometry

The X-ray diffraction (XRD) diffractograms were obtained at room temperature with a Philips PM9901/00 diffractometer (Philips). The measurement conditions were  $\text{CuK}_\alpha$  target; nickel filter; 40 kV voltage; 20-mA current; 0.1-mm slit; and  $2^\circ/\text{min}$  scanning speed. Approximately 200 mg of powder was loaded into an aluminum sample holder, taking care not to introduce a preferential orientation of the crystals. Crystals were ground into a powder with average particle size below  $250 \mu\text{m}$ . Grinding did not change the crystal form.

### Differential Scanning Calorimetry

For differential scanning calorimetry (DSC), a Shimadzu DSC-50 was used to obtain DSC thermograms of the different powders. A mass not exceeding 3.0 mg was measured into aluminum crimp cells. DSC curves were obtained at a heating rate of  $10^\circ\text{C}$  per min under a nitrogen purge of 30 ml per min.

### Solubility

The different powders were sieved using a  $250\text{-}\mu\text{m}$  sieve. Amounts large enough to ensure that supersaturation could be obtained were measured in test tubes with screw caps. To each test tube, 5 ml distilled water was added, and the caps were screwed on tightly. The test tubes were rotated at 60 rpm (Heidolph RZR-2000 rotator, Kelheim, West Germany) in a thermostatically (Julabo EM thermostat, Seelbach, West Germany) controlled water bath at  $30^\circ\text{C} \pm 1^\circ\text{C}$  for 24 hr. The concentrations of the filtered samples were determined spectrophotometrically.

Standard solutions of rifampicin within the concentration range 0.5 to  $20 \mu\text{g/ml}$  were prepared, and the absorbances were measured at 333 nm using a Beckman DU 650I UV-visible recording spectrophotometer. A standard curve was plotted ( $r = 0.9998$ ) using the acquired data. From the absorbance of the filtered samples and using the values of the standard curve

(slope = 0.0353;  $Y$  intercept = 0.0010), the solubility was calculated.

### Powder Dissolution Measurements

Powder dissolutions were performed according to the method described by Lötter et al. (5) using apparatus no. 2 (Vankel VK 700, USA) of the USP (6,7). Water, 0.1 M HCl, or phosphate buffer pH 7.4 containing 0.1 M  $\text{NaH}_2\text{PO}_4$  and 0.1 M  $\text{Na}_2\text{HPO}_4 \cdot \text{H}_2\text{O}$ , thermostatically controlled at  $37^\circ\text{C} \pm 0.5^\circ\text{C}$  (Vankel VK 650A), were used as dissolution media. Before dissolution, the rifampicin powder was mixed with glass beads (0.1–0.11 mm in diameter) and vortexed. This was introduced into the 900 ml of dissolution medium, stirred at 100 rpm. Samples were withdrawn at 1, 2, 4, 8, 16, 32, and 64 min through a 0.2- $\mu\text{m}$  membrane filter. The amount of dissolved rifampicin was determined spectrophotometrically. Similarities among the dissolution curves were calculated using an equation described by Moore and Flanner (7).

## RESULTS AND DISCUSSION

Visual inspection of the raw materials with SEM showed definite differences in their particle sizes and shapes. Crystals of powder A, with a mean particle size of 164  $\mu\text{m}$  were “bricklike” to elongated with even sides (Fig. 1a). The particles of powder B were not well defined, but had a smooth surface, with a mean particle size of 107  $\mu\text{m}$  (Fig. 1b). Sample C was a mixture of “rod-like” to shapeless particles with a mean diameter of 95  $\mu\text{m}$  (Fig. 1c). Particles of sample D were characterized by uneven surfaces and a mean particle size of 147  $\mu\text{m}$  (Fig. 1d). The crystals of sample E were rodlike with a mean particle size of 170  $\mu\text{m}$  (Fig. 1e). This powder contained a large percentage of very fine particles with a mean size below 30  $\mu\text{m}$ .

These differences prompted closer investigation into the specific crystal forms. Pelizza et al. reported the characterization of rifampicin crystals using IR spectroscopy (2). Therefore, IR spectra (Fig. 2) of the samples were taken, and the IR spectra were compared based on the principles discussed by Pelizza et al. From these comparisons, powders A, B, and E were characterized as form II of Pelizza et al. Powders C and D were a mixture of form II and an amorphous form.

For all the powders (Fig. 2), the normally sharp band for the NH group was not present, indicating intramolecular bonding between the NH group and the piperazine side chain. The broad band assigned to the  $\nu$  OH was

present; thus,  $\text{C}_1=\text{O}$  chelated with the  $\text{C}_8$  hydroxyl group. The band at  $798\text{ cm}^{-1}$  associated with the chromophore moiety ring vibrations was also present in all the powders. The presence of the vibration due to the  $\nu\text{ C}=\text{O}$  group explained the hydrogen bonding of the  $\text{C}_{23}-\text{OH}$  to the acetyl group on  $\text{C}_{25}$  in all five powders.

The best indication of polymorphism are differences in the XRD patterns (Fig. 3) of powders. Comparison with XRD patterns reported by Pelizza et al. indicated that powders A, B, and E were the same as form II, with main XRD peaks at  $19.92^\circ$ ,  $15.89^\circ$ , and  $12.71^\circ$   $2\theta$  (2). Slight differences in  $d$  spacings and corresponding relative intensities between the results of Pelizza et al. and those reported here could be because different X-ray powder diffractometers and measurement conditions were used.

The main peaks characteristic of form II at  $19.92^\circ$ ,  $15.89^\circ$ , and  $12.71^\circ$   $2\theta$  were also present in the X-ray diffractogram of powders C and D (Fig. 3). However, a sharp drop in peak intensity counts from about 6400–10,000 to 1225–1600 indicated that a large percentage of a less crystalline form was present in these powders. Most probably, powders C and D were mixtures of an amorphous form and form II.

DSC can also identify polymorphism. Since this is an easy method available to most pharmaceutical manufacturers, it was also used to characterize the rifampicin powders. The DSC thermograms of rifampicin raw materials are shown in Fig. 4. The general appearance of the thermograms was the same, although slight differences in peak sizes and positions were observed.

Again, thermograms of powders A, B, and E were similar (Fig. 4), and the thermograms were comparable with that reported for form II (8). These powders showed an endotherm at  $188^\circ\text{C}$ – $193^\circ\text{C}$ , corresponding to melting of the powder. It was immediately followed by an exotherm, which corresponded to recrystallization of the melt. The melt decomposed exothermally at around  $250^\circ\text{C}$ . Thermograms of powders C and D were similar to the thermograms of samples A, B, and E (Fig. 4), except that the melting endotherm was at a distinctly lower temperature ( $177^\circ\text{C}$ – $178^\circ\text{C}$ ). The temperature at which decomposition occurred was reduced to around  $239^\circ\text{C}$  for powders C and D.

Pelizza et al. reported that rifampicin predominantly crystallizes as a hydrate with varying numbers of water molecules incorporated into the crystal structure (2). Frequently, hydrates and crystals containing volatile solvents are changed to noncrystalline amorphous powders on drying. This can lead to a significant decrease in the temperature of decomposition, as observed for powders C and D. Based on this, DSC changes confirmed the pres-

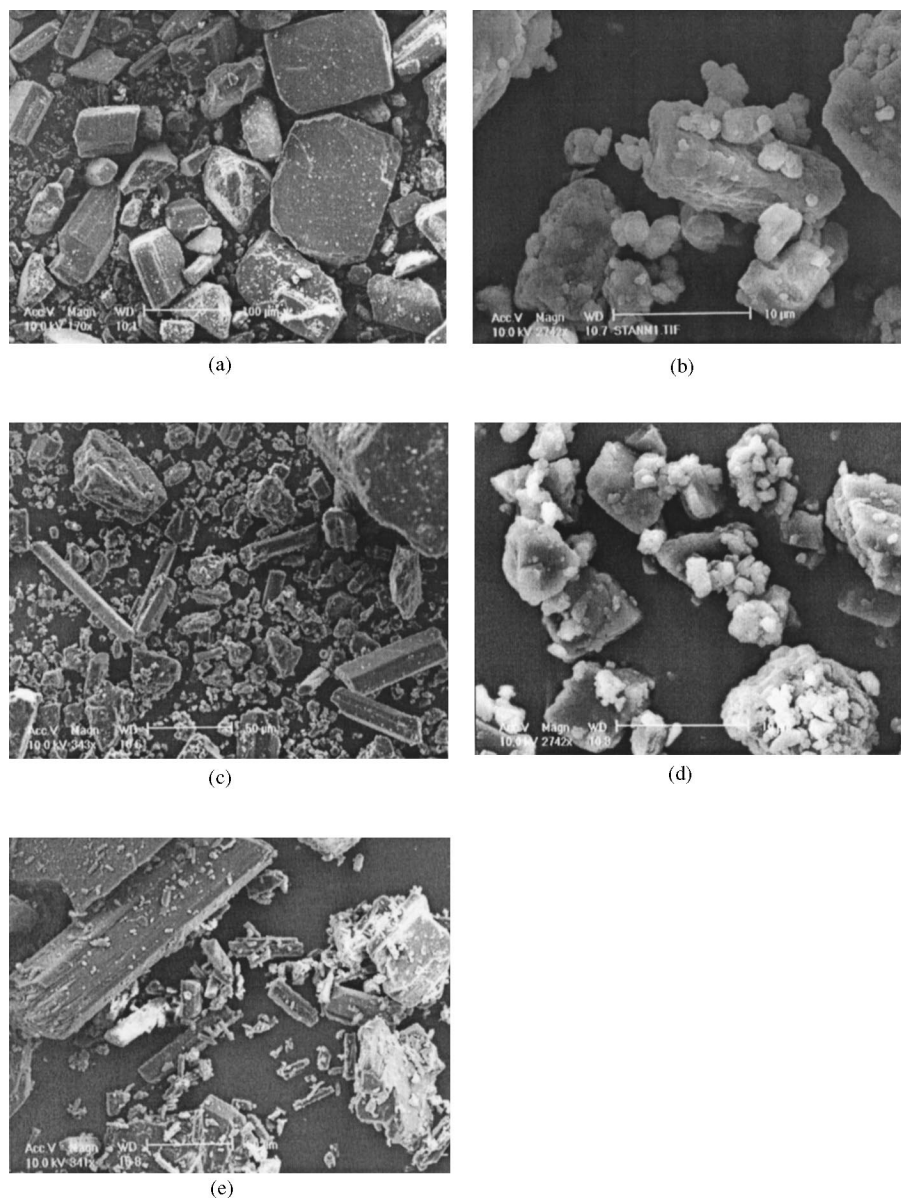


**Figure 1.** Scanning electron photomicrographs of different rifampicin powders: (a) A, (b) B, (c) C, (d) D, and (e) E.

ence of a substantial amount of an amorphous form present in samples C and D. Therefore, it proved a useful method to identify the presence of an amorphous form in rifampicin powders.

Since it is well known that changes in polymorphic forms can change the solubility and dissolution properties of a drug, the solubilities and dissolution behaviors of the different rifampicin powders were also measured. The re-

sults listed in Table 1 indicated that the solubilities of the powders identified as form II (A, B, and E) were less in water at 30°C than the solubilities of the powders containing a significant amount of amorphous material (C and D). Powder A, characterized as form II, was slightly more soluble than the other two form II powders, 1.61 mg/ml versus 1.51 mg/ml. This slight difference might be due to a small amount of amorphous material present

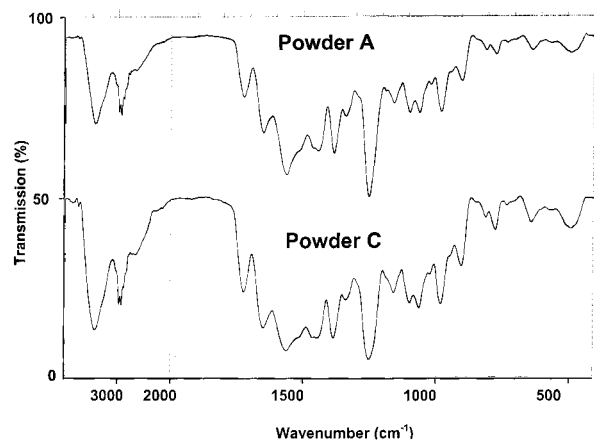


**Figure 2.** IR spectra of powders A (form II) and C (form II and an amorphous form).

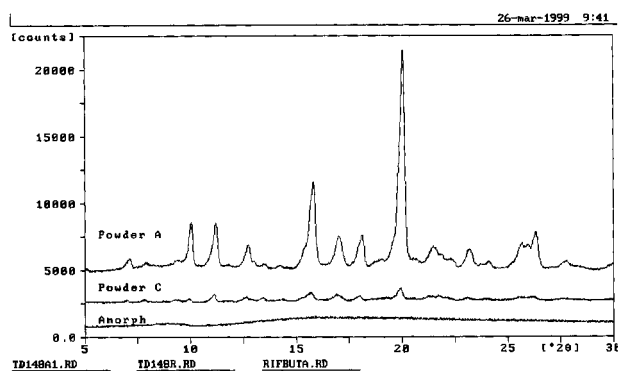


**Figure 3.** XRD diffractograms of powders A and C and an amorphous form.

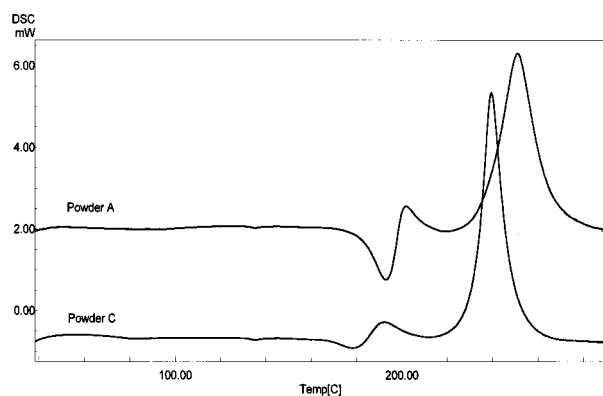


**Figure 4.** DSC thermograms of powders A and C.

**Table 1**  
*Solubility of Rifampicin Raw Materials in Water*

Sample	Crystal Form	Solubility mg/ml
A	II	$1.61 \pm 0.05$
B	II	$1.51 \pm 0.05$
C	Mixture of form II and the amorphous form	$1.74 \pm 0.07$
D	Mixture of form II and the amorphous form	$1.71 \pm 0.03$
E	II	$1.51 \pm 0.07$

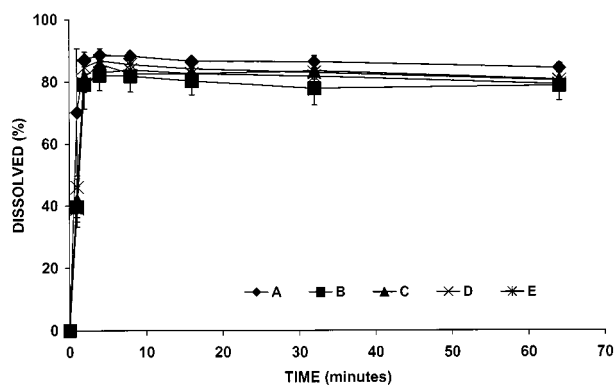


**Figure 5.** Dissolution profiles of the different rifampicin powders in 0.1 M HCl.

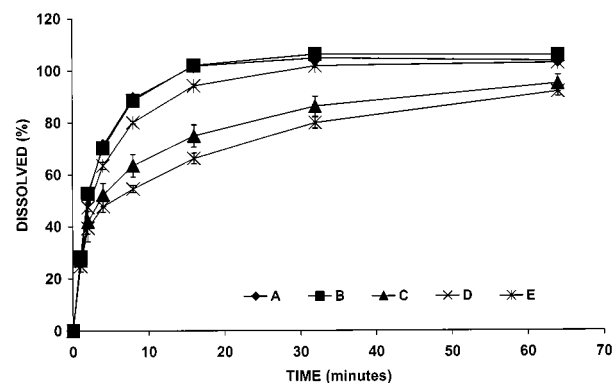


**Figure 6.** Dissolution profiles of the different rifampicin powders in phosphate buffer pH 7.4.



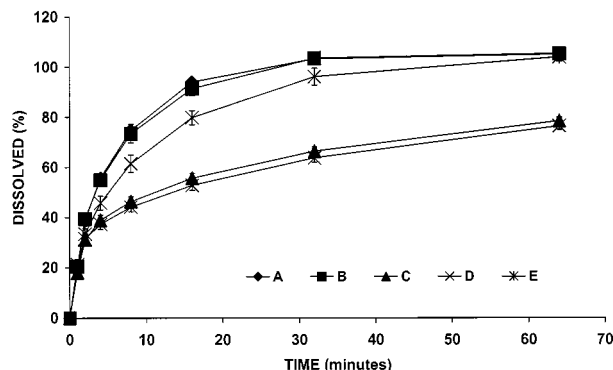


**Figure 7.** Dissolution profiles of the different rifampicin powders in water.

in sample A. This was confirmed by a decrease in maximum counts at the 100%  $I/I_0$  peak in the XRD diffractogram of powders B (8000) and E (10,000), to about 6400 for powder A.

The dissolution profiles of the powders in 0.1 M HCl, buffer pH 7.4, and water are shown in Figs. 5, 6, and 7, respectively. Similarity factors  $f_2$  calculated showed that the dissolution profiles of rifampicin powders in 0.1 M HCl were within 10% of each other and therefore were similar (mean  $f_2 = 67.9 \pm 15.9$ ). In buffer at pH 7.4, powders A, B, and E (mean  $f_2 = 74.4 \pm 15.6$ ) and powders C and D ( $f_2 = 65.1$ ) had similar dissolution profiles, respectively, but the profiles of powders C and D were not similar to those of A, B, and E (mean  $f_2 = 0.2 \pm 5.1$ ). The slower dissolutions of powders C and D were even more pronounced in water (mean  $f_2 = 35.0 \pm 3.6$ ). This result was not expected since it is generally thought that amorphous materials are more soluble than crystals.

To substantiate the poor dissolution of less crystalline rifampicin, amorphous rifampicin (Fig. 3) was prepared as described by Pelizza et al., and the dissolution properties were measured (Figs. 5, 6, and 7) (2). The amorphous powders dissolved very poorly and were not at all similar to form II ( $f_2 = 12.84$ ).

## CONCLUSIONS

The results of this study showed that the physical properties of rifampicin raw materials varied not only

among manufacturers, but also among batches of the same manufacturer. The main difference among the powders was the amorphous content. The presence of amorphous rifampicin could be detected by XRD, IR, and DSC methods. Although the amorphous powders (C and D) were more soluble than those of crystalline form II (powders A, B and E), it did not lead to improved dissolution. In fact, contrary to expectations, an increase in amorphous content significantly reduced the dissolution rate of the powders in water and buffer pH 7.4. This behavior was attributed to the electrostatic properties of the very fine particles in the amorphous powders. Electrostatic forces resulted in lump formation, which was observed during dissolution testing.

## ACKNOWLEDGMENTS

The authors would like to thank the FRD for their financial support during this study and Hoechst Marion Roussel (South Africa) for supplying the rifampicin raw materials.

## REFERENCES

1. P. T. Mannisto, *Clin. Pharmacol. Ther.*, 21, 370–394 (1977).
2. G. Pelizza, M. Nebuloni, P. Ferrari, and G. G. Gallo, *Il Farmaco Ed.*, 32, 471–481 (1977).
3. S. R. Byrn, *Solid-State Chemistry of Drugs*, Academic, New York, 1982.
4. K. C. Jindal, R. S. Chaudhary, A. K. Singla, S. S. Gangwal, and S. Khanna, *Pharm. Ind.*, 57, 420–422 (1995).
5. A. P. Lötter, D. R. Flanagan, N. R. Palepu, and J. K. Guilory, *Pharm. Technol.*, 7, 55–66 (1983).
6. U.S. Pharmacopeial Convention, *United States Pharmacopeia*, 23<sup>rd</sup> ed., Author, Rockville, Maryland, 1995, p. 2391.
7. J. W. Moore and H. H. Flanner, *Pharm. Technol.*, 20, 64–74 (1996).
8. G. G. Gallo and P. Radaelli, in *Analytical Profiles of Drug Substances*, Vol. 5 (K. Florey, Ed.), Academic, New York, 1976, p. 560.



Copyright of Drug Development & Industrial Pharmacy is the property of Taylor & Francis Ltd and its content may not be copied or emailed to multiple sites or posted to a listserv without the copyright holder's express written permission. However, users may print, download, or email articles for individual use.